0026-895X/02/6102-455–462$3.00
MOLECULAR PHARMACOLOGY
Vol. 61, No. 2
1238/965671
Mol Pharmacol 61:455–462, 2002
Printed in U.S.A.

Human A_{2A} Adenosine Receptors: High-Affinity Agonist Binding to Receptor-G Protein Complexes Containing $G\beta_4$

LAUREN J. MURPHREE, MELISSA A. MARSHALL, JAYSON M. RIEGER, TIMOTHY L. MACDONALD, and JOEL LINDEN

Departments of Pharmacology (L.J.M.), Medicine (M.A.M., J.L.), and Chemistry (J.M.R., T.L.M.), University of Virginia, Charlottesville, Virginia

Received July 26, 2001; accepted October 10, 2001

This paper is available online at http://molpharm.aspetjournals.org

ABSTRACT

Agonists bind with higher affinity to G protein-coupled heptahelical receptors than to uncoupled receptors. Recombinant A_1 and A_3 adenosine receptors couple well to $G_{i/o}$, but recombinant human A_{2A} adenosine receptors ($hA_{2A}AR$) couple poorly to G_s and bind agonists with K_i values in binding assays that are much higher than ED_{50} values for functional responses such as coronary dilation and inhibition of neutrophil oxidative burst. In this study, we produced $hA_{2A}AR$-G protein complexes in membranes derived from Sf9 cells quadruply infected with receptors and heterotrimeric G protein subunits. The composition of G_β markedly influences coupling such that $A_{2A}AR$-$\alpha_s\beta_1\gamma_2$ are 8 ± 2% coupled whereas equivalently expressed $A_{2A}AR$-$\alpha_s\beta_4\gamma_2$ are 40 ± 2% coupled. Hence, we were able for the first time to accurately measure high-affinity agonist binding to $hA_{2A}AR$. The agonist 2-[2-(4-amino-3-[^{125}I]iodophenyl)ethylamino]adenosine binds to coupled and uncoupled $hA_{2A}AR$ with K_D values of 0.46 nM and 26 nM, respectively, a difference in affinity of 57-fold. The addition of GTPγS converts all receptors to the low-affinity state. $A_{2A}AR$ coupling does not influence binding of antagonists including, ^{125}I-4-(2-[7-amino-2-[2-furyl][1,2,4]triazolo[2,3-*a*][1,3,5]triazin-5-yl-amino]ethyl)phenol (^{125}I-ZM241385), K_D = 0.5 nM. Based on a comparison of high-affinity binding sites, N^6-3-iodo-2-chlorobenzyladenosine-5′-*N*-methyluronamide is only 8-fold A_3 selective ($A_{2A\ Ki,\ H}$ = 18.3 ± 3.2 nM; $A_{3\ Ki,\ H}$ = 2.4 ± 0.3 nM) and 2-chloro-N^6-cyclopentyladenosine is only 33-fold A_1 selective ($A_{2A\ Ki,\ H}$ = 11.0 ± 1.9; $A_{1\ Ki,\ H}$ = 0.3 ± 0.1). We conclude that recombinant $hA_{2A}AR$ can form a high-affinity receptor-G protein complex with $\alpha_s\beta_4\gamma_2$ that is useful for determining receptor selectivity.

A_{2A}ARs are one of four subtypes (A_1, A_{2A}, A_{2B}, and A_3) of GPCRs that respond to the purine adenosine, which is released from tissues in response to metabolic stress or ischemia. The A_{2A}AR is an important pharmacological target because of the generally anti-inflammatory effects elicited when it is activated (Sullivan and Linden, 1998; Linden, 2001). Like other GPCRs, the A_{2A}AR population is composed of receptors in two conformational states: those coupled to a heterotrimeric G protein, forming an R-G complex, and those that are uncoupled. GPCRs can be converted to uncoupled receptors upon binding of guanine nucleotides such as GTPγS to the G protein. Coupled GPCRs have a higher affinity for agonist molecules than do their uncoupled counterparts.

We have shown previously that the radiolabeled agonist [^{125}I]APE binds to two affinity states of rat striatal A_{2A} adenosine receptors (K_D = 1.3 and 19 nM) and < 20% of striatal receptors are found in the high-affinity conformation (Luthin et al., 1995). [^{3}H]CGS21680 also binds to two affinity states of rat striatal membranes (K_D = 3.9 and 51 nM) (Luthin et al., 1995) and to two affinity states in human brain preparations (Wennmalm, 1988). The high-affinity state of the recombinant human A_{2A}AR has not been easily observable because recombinant A_{2A}ARs do not seem to form R-G complexes to a significant degree. Poor A_{2A} coupling was noted in COS-7 cells assayed with [^{125}I]APE (Luthin et al., 1995) and in Chinese hamster ovary cells assayed with [^{3}H]NECA (Klotz et al., 1998). Similarly, little GTPγS-sensitive [^{3}H]CGS21680 binding is detected to A_{2A}ARs transfected into COS-7 cells or human embryonic kidney 293 cells, suggesting that few receptors are coupled to G proteins (Piersen et al., 1994; Rosin et al., 1996). The inability to detect the high-affinity agonist binding conformation of the $hA_{2A}AR$ may have resulted in an underestimation of the relative

This work was supported in part by National Institutes of Health Grants R01-HL37942 (J.L.).

ABBREVIATIONS: A_{2A}AR, A_{2A} adenosine receptor; GPCR, G protein coupled receptor; [^{125}I]APE, 2-[2-(4-amino-3-[^{125}I]iodophenyl)ethylamino-]adenosine; CGS21680, 2-[4-(2-carboxyethyl)phenethylamino]-5′-*N*-ethylcarboxamidoadenosine; GTPγS, guanosine-5′-*O*-(3-thio)triphosphate; ZM241385, 4-(2-[7-amino-2-[2-furyl][1,2,4]triazolo[2,3-*a*][1,3,5]triazin-5-yl-amino]ethyl)phenol; ATL146e, 4-{3-[6-Amino-9-(5-ethylcarbamoyl-3,4-dihydroxy-tetrahydro-furan-2-yl)-9*H*-purin-2-yl]-prop-2-ynyl}-cyclohexanecarboxylic acid methyl ester; MRS 1220, *N*-(9-chloro-2-furan-2-yl-[1,2,4]triazolo[1,5-*c*]quinazolin-5-yl)-2-phenylacetamide; NECA, 5′-*N*-ethylcarboxamidoadenosine; XAC, 8-(4-((2-a-minoethyl)aminocarbonylmethyloxy)phenyl)-1–3-dipropylxanthine; CPA, N^6-cyclopentyladenosine; IB-MECA, N^6-3-iodobenzyladenosine-5′-*N*-methyluronamide, PMSF, phenylmethylsulfonyl fluoride; TBST, Tris-buffered saline/Tween 20; HE, HEPES/EDTA; [^{125}I]ABA, N^6-(4-amino-3-[^{125}I]iodo-benzyl)adenosineC-CPA, 2-chloro-N^6-cyclopentyladenosine; Cl-IB-MECA, N^6-3-iodo-2-chlorobenzyladenosine-5′-*N*-methyluronamide.

affinity of agonists for $hA_{2A}AR$ compared with hA_1ARs and hA_3ARs (Sullivan et al., 2001).

The composition of G protein β-subunits influences the potency of $\beta\gamma$ to stimulate guanine nucleotide exchange in assays with $A_{2A}AR$-G protein complexes such that $G\beta_4$ is more potent than $G\beta_1$ (McIntire et al., 2001). This prompted us investigate the influence of G protein β-subunit composition on the degree of coupling to recombinant A_{2A} receptors. Recombinant baculoviruses encoding the $hA_{2A}AR$ and three heterotrimeric G protein subunits were overexpressed in Sf9 cells. Expression of $\alpha_s\beta_4\gamma_2$ with $hA_{2A}AR$ results in well-coupled receptors. We have used membranes from these Sf9 cells to investigate the affinities of various agonists for the high-affinity conformational state of $hA_{2A}ARs$.

Experimental Procedures

Materials. ZM241385 (Poucher et al., 1995) was a gift from Simon Poucher (Astra-Zeneca Pharmaceuticals, Cheshire, UK). Carrier-free ^{125}I-ZM241385 and [^{125}I]APE were synthesized and purified using high-performance liquid chromatography as described previously (Linden et al., 1984; Sullivan et al., 1999). ATL 146e was prepared as described previously (Rieger et al., 2001). MRS 1220 (Jacobson, 1998) was a gift from Kenneth Jacobson (National Institutes of Health; Bethesda, MD). CGS21680, NECA, XAC, CPA, and IB-MECA were purchased from Sigma/RBI (Natick, MA).

CCPA was purchased from SRI (Menlow Park, CA). ABA was a gift from Susan Daluge (GlaxoSmithKline, Research Triangle Park, NC). Adenosine deaminase was purchased from Boehringer Mannheim Biochemicals (Indianapolis, IN). Cell culture media and reagents were purchased from Invitrogen (Carlsbad, CA). The following reagents were purchased from Sigma Chemical Co. (St. Louis, MO): GTPγS, GDP, PMSF, leupeptin, pepstatin, aprotinin, and theophylline. Recombinant baculoviruses encoding the G protein subunits α_s, β_1, β_4, and γ_2 were kindly provided by James C. Garrison at the University of Virginia. The baculovirus encoding the $hA_{2A}AR$ was constructed as described previously (Robeva et al., 1996).

Cell Culture and Membrane Preparation. Sf9 cells were cultured in Grace's medium supplemented with 10% fetal bovine serum, 2.5 μg/ml amphotericin B, and 50 μg/ml gentamycin in an atmosphere of 50% N_2/50% O_2. Viral infection was performed at a density of 2.5×10^6 cells/ml with a multiplicity of infection of two for each virus used. Infected cells were harvested 3 days postinfection and washed twice in insect PBS, pH 6.3. Cells were then resuspended in lysis buffer [20 mM HEPES, pH 7.5, 150 mM NaCl, 3 mM $MgCl_2$, 1 mM β-mercaptoethanol, 5 μg/ml leupeptin, 5 μg/ml pepstatin A, 1 μg/ml aprotinin, and 0.1 mM PMSF] and snap-frozen for storage at −80°C. Cells were thawed on ice, brought to 30 ml of total volume in lysis buffer, and burst by N_2 cavitation (600 psi for 20 min). A low-speed centrifugation was performed to remove any unlysed cells (1000*g* for 10 min), followed by a high-speed centrifugation (17,000*g* for 30 min). The pellet from the final centrifugation was homogenized in buffer containing 20 mM HEPES, pH 8, 100 mM NaCl, 1% glycerol, 2 μg/ml leupeptin, 2 μg/ml pepstatin A, 2 μg/ml aprotinin, 0.1 mM PMSF, and 10 μM GDP using a small glass homogenizer followed by passage through a 26-gauge needle. Membranes were aliquoted, snap frozen in liquid N_2, and stored at −80°C. Membranes from cells stably expressing the human A_1 AR (Chinese hamster ovary K1 cells) or A_3 AR (human embryonic kidney 293 cells) were prepared as described previously (Robeva et al., 1996).

Western Blotting. For each membrane preparation, 100 μg of membrane protein was added to 2× electrophoresis buffer (20% glycerol, 150 mM Tris, 0.05 mg/ml bromphenol blue, 4% SDS) plus 1 mM β-mercaptoethanol, loaded onto 10% Tris-Glycine Gradigels and electrophoresed at a constant voltage of 150 V for 90 min. Samples were transferred onto Westran polyvinylidene difluoride membranes (Schleicher and Schuell) using a constant current of 150 mA for 90 min. Nonspecific sites were blocked by incubating blots overnight at 4°C in a solution of TBST (50 mM Tris, 150 mM NaCl, and 0.5% Tween 20) containing 5% milk at pH 8. Blots were rinsed 4 × 5 min in TBST and then incubated with the primary antibody (NEN808 for β_{common} and NEI800 for α_{common}) in 2% milk in TBST. Blots were again rinsed 4 × 5 min with TBST before incubating for 90 min with donkey anti-rabbit IgG-horseradish peroxidase-linked $F(ab')_2$ at a dilution of 1:3000. Blots were rinsed 3 × 5 min in TBST, exposed to enhanced chemiluminescence reagents for 1 min, and placed on Kodak X-ray film for 15 s.

Radioligand Binding Assays. Radioligand binding to recombinant human A_{2A} receptors in Sf9 cell membranes was performed using either the radiolabeled agonist [^{125}I]APE (Luthin et al., 1995) or the radiolabeled antagonist ^{125}I-ZM241385. To detect the high-affinity, GTPγS-sensitive state of A_1 and A_3 AR, we used the agonist [^{125}I]ABA (Linden et al., 1985, 1993). Binding experiments were performed in triplicate with 5 μg (A_{2A}) or 25 μg (A_1 and A_3) membrane protein in a total volume of 0.1 ml HE buffer (20 mM HEPES and 1 mM EDTA) with1 U/ml adenosine deaminase and 5 mM $MgCl_2$ with or without 50 μM GTPγS. Membranes were incubated with radioligands at room temperature for 3 h (for agonists) or 2 h (for antagonists) in Millipore Multiscreen 96-well GF/C filter plates and assays were terminated by rapid filtration on a cell harvester (Brandel, Gaithersburg, MD) followed by four 150-μl washes over 30 s with ice-cold 10 mM Tris-HCl, pH 7.4, 10 mM $MgCl_2$. Nonspecific binding was measured in the presence of 50 μM NECA. For binding isotherms, nonspecific binding and free radioligand were fit by least-squares regression to a straight line. The extrapolated fit value of nonspecific binding for each free concentration of radioligand was subtracted from total binding to calculate specific binding. Equilibrium binding assays using [^{125}I]APE were carried out using isotope dilution (100 nM unlabeled I-APE and 5 nM [^{125}I]APE before serial dilutions) to create a range of radioligand concentrations useful for detecting both high- and low-affinity binding sites. Saturation binding assays using ^{125}I-ZM241385 did not require isotope dilution. B_{max} and K_D values were fit using nonlinear least-squares interpolation (Marquardt, 1963) for single or two-site binding models. For curvilinear 2-site Scatchard analyses (plots of $[L]_{bound}$ versus $[L]_{bound}/[L]_{free}$), $[L]_{bound}/[L]_{free}$ was calculated from specific binding using the quadratic equation $Y = -B + (\sqrt{B^2 - 4AC}) / 2A$, where $Y = [L]_{bound}/[L]_{free}$, $A = K_{D1} \times K_{D2}$, $B = X(K_{D1} + K_{D2}) - B_{max1} \times K_{D2} - B_{max2}$, $C = X \times (X - B_{max1} - B_{max2})$, and X = specific binding. Optimal parameter values were determined by nonlinear least-squares interpolation.

Competition binding assays were performed as described previously (Robeva et al., 1996) using 0.5 to 1 nM [^{125}I]APE, ^{125}I-ZM241385, or [^{125}I]ABA. We found that it was sometimes important to change pipette tips after each serial dilution to prevent transfer on tips of potent hydrophobic compounds. The K_i values for competing compound binding to a single site were derived from IC_{50} values with correction for radioligand and competing compound depletion as described previously (Linden, 1982). For determining two K_i values for agonists in competition for an antagonist radioligand binding with the same affinity to both sites, we used nonlinear least-squares fitting to solve three simultaneous equations:

$$B_L = \frac{B_{L1}}{1 + C_f/K_{i1} + L_f/K_D} + \frac{B_{L2}}{1 + C_f/K_{i2} + L_f/K_D} + f \times L_f$$

$B_L = L_T - L_f$, and $B_C = C_T - C_f$, where B_L represents bound radioligand, B_C is bound competitor, L_T and L_f represent total and free radioligand, C_T and C_f represent total and free competitor, f is the ratio of nonspecific binding to L_f, and K_D is known from independent binding isotherms.

To determine the rate of association of [^{125}I]APE to $A_{2A}AR$-$\alpha_s\beta_4\gamma_2$, 50 μl of membrane protein solution (0.03 mg/ml membrane protein in

HE buffer containing 2 U/ml adenosine deaminase) was dispensed onto filter plates. At various time points, 50 μl of radioligand solution (0.68 nM [^{125}I]APE in HE buffer containing 10 mM $MgCl_2$) was added to the membrane solution yielding final concentrations of 0.34 nm [^{125}I]APE and 5 mM $MgCl_2$. The experiment was terminated by rapid filtration as described above. For determination of dissociation kinetics, radioligand, and membrane solution were dispensed into filter plates and allowed to incubate for 3 h. Dissociation was started by addition of 50 μl of HE buffer containing 5 mM $MgCl_2$ and 50 μM ZM241385 at various time points followed by rapid filtration.

Results

To produce membranes containing $hA_{2A}AR$ that are partially coupled to G proteins, Sf9 cells were simultaneously infected with a baculovirus encoding the $hA_{2A}AR$ or four baculoviruses encoding the receptor and the heterotrimeric G protein subunits α_s, β_2 or β_4, and γ_2. The amount of receptor expression was determined from saturation binding isotherms using both the agonist [^{125}I]APE and the antagonist ^{125}I-ZM241385 as radioligands. The data from antagonist saturation experiments (found in Table 1) shows that the neither the presence of G proteins nor addition of GTPγS significantly changed the B_{max} for ^{125}I-ZM241385.

The data from agonist saturation binding summarized in Table 1 shows that the A_{2A} receptor, when expressed alone, has a relatively low affinity for [^{125}I]APE (K_D = 27 nM). Scatchard analysis indicates that all agonist binding is optimally fit to a single affinity site. When G proteins are coexpressed, the receptor displays two different affinities for the agonist. Table 1 shows that Gβ_1- and Gβ_4-containing membranes have similar high-affinity (K_H) binding dissociation constants for [^{125}I]APE of 0.32 nM and 0.46 nM, respectively. The low-affinity (K_L) dissociation constants also are similar (K_L = 10.5 nM and K_L = 26 nM). Neither K_H nor K_L are significantly different between membranes expressing Gβ_1 or Gβ_4.

The total number of receptors measured varied with the choice of ligand. The B_{max} using ^{125}I-ZM241385 is significantly greater than that using [^{125}I]APE. This is probably caused by partial dissociation of the agonist ligand from the low-affinity site during washing of glass fiber filters. This phenomenon would cause the low-affinity B_{max} values to appear artificially depressed without affecting the observed K_D. Thus, to determine the fraction of receptors found in the high-affinity state, we divided the high-affinity B_{max} by the total number of receptors as determined by saturation binding of ^{125}I-ZM241385 ($B_{max,\ ZM}$). This analysis shows that the Gβ subunit influences the efficiency of R-G coupling in this system. The fraction of receptors found in the high-affinity state in the presence of Gβ_4 (40%) was significantly higher than that seen when β_1 was present (8%) (Table 1). This difference cannot be attributed to a difference in the amount of expressed α- or β-subunits, because the amount of protein detected in Sf9 membranes by Western blotting with antibodies that detect α or β subunits was similar (Fig. 1). The anti-β antibody detects β_1 and β_4 with the same affinity because it recognizes a common epitope. Because the Gβ_4-containing membranes had a greater fraction of coupled receptors, we used them to characterize agonist high-affinity binding sites in subsequent experiments.

The equilibrium binding of [^{125}I]APE to membranes derived from Sf9 cells quadruply infected with $hA_{2A}AR$-$\alpha_s\beta_4\gamma_2$ complexes with or without GTPγS is shown in Fig. 2A. Coinfection with G protein subunits substantially increased the amount of specific binding at a given concentration without changing nonspecific binding. In the absence of GTPγS, specific binding to R-G complexes is fit significantly better to a two-site binding model (Fig. 2A, —■—) than to a single site equation (Fig. 2A, - - ■ - -). The two [^{125}I]APE affinity states of $hA_{2A}AR$-$\alpha_s\beta_4\gamma_2$ complexes are more clearly evident in the Scatchard plot shown in Fig. 2B. Treatment of membranes expressing these receptor-G protein complexes with GTPγS (50 μM) eliminates the high-affinity site completely, resulting in equilibrium binding that is optimally fit to a single-site equation (K_D = 32 nM) and characterized by a linear Scatchard plot. This affinity is similar to the low-affinity population of receptors detected in the absence of GTPγS (26 nM) or the single low-affinity site detected when the receptor is expressed alone (27 nM). This GTPγS sensitivity of binding confirms that the high-affinity site is due to the interaction of the receptor with G proteins.

We next conducted kinetic experiments to determine k_1 and k_{-1} for [^{125}I]APE binding $hA_{2A}AR$-$\alpha_s\beta_4\gamma_2$ complexes. The kinetics of [^{125}I]APE (0.34 nM) association is illustrated in Fig. 3A. At this concentration, [^{125}I]APE binds with a k_{obs} of 0.0673 ± 0.0025 min^{-1}. The binding is well fit by a single exponential equation, which is confirmed by the linearity of the transformed data shown in the Fig. 3, inset. The slope of this line defines a pseudo–first-order rate constant (k_1 × [[^{125}I]APE] + k_{-1}) and is calculated based on the assumption that free radioligand does not change significantly over time. During this experiment, only 15% of the radioligand was

TABLE 1

Saturation binding parameters of $hA_{2A}AR$ expressed with or without G proteins

Binding parameters of a selective A_{2A} antagonist (^{125}I-ZM241385) or agonist ([^{125}I]APE) to Sf9 cell membranes expressing A_{2A} receptors with or without G proteins (α_s,β_4 or β_1,γ_2) and in the presence or absence of 50 μM GTPγS as described in *Experimental Procedures*. K_H and K_L represent the K_D values of the high- and low-affinity states, respectively. The percentage of coupled receptors is determined by dividing the number of receptors in the high-affinity state ($B_{max,H}$) by the total number of receptors (B_{max} for ^{125}I-ZM241385). Values represent means ± S.E.M.; n = 3 to 5.

Membrane	^{125}I-ZM241385 Binding		[^{125}I]APE Binding				Coupled
	K_D	B_{max}	K_H	$B_{max,H}$	K_L	B_{maxL}	
	nM	*fmol/mg*	*nM*	*fmol/mg*	*nM*	*fmol/mg*	%
A_{2A}	0.45 ± 0.07	25,775 ± 3,731	N.A.	N.A.	27 ± 2.8	17,095 ± 1,300	N.A.
A_{2A} + GTPγS	0.55 ± 0.02	24,635 ± 2,000	N.A.	N.A.	31 ± 3.6	13,300 ± 280	N.A.
A_{2A} + $\alpha_s\beta_{1\gamma2}$	0.51 ± 0.01	23,425 ± 380	0.32 ± 0.2	1950 ± 500	10.5 ± 5.5	8,749 ± 3,831	8 ± 2
A_{2A} + $\alpha_s\beta_{1\gamma2}$ + GTPγS	N.D.	N.D.	N.A.	N.A.	20.5 ± 0.5	6,422 ± 1,000	N.A.
A_{2A} + $\alpha_s\beta_{4\gamma2}$	0.49 ± 0.07	23,390 ± 100	0.46 ± 0.1	9410 ± 500	26 ± 6.0	22,000 ± 690	40 ± 8
A_{2A} + $\alpha_s\beta_{4\gamma2}$ + GTPγS	0.53 ± 0.06	22,050 ± 250	N.A.	N.A.	32 ± 2.5	15,000 ± 2,000	N.A.

N.A., not applicable; N.D., not done.

bound at equilibrium. The dissociation of [^{125}I]APE is shown in Fig. 3B. The data is well fit by a single exponential equation, which is consistent with the proposition that a large fraction of the total binding is to the high-affinity site. We calculated k_{-1} to be 0.0291 ± 0.002 min^{-1} corresponding to a $t_{1/2}$ of 24 min. A kinetic analysis of [^{125}I]APE dissociation from the low-affinity site could not be accurately performed because of rapid dissociation of the radioligand.

From k_{obs} and k_{-1} of the high-affinity site, and using (k_{obs} = $k_1 \times$ [[^{125}I]APE]+ k_{-1}) we calculated k_1 as $1.12 \times 10^8 \pm 0.09 \times 10^8$ min/M. The K_D for [^{125}I]APE was calculated ($K_D = k_{-1}/k_1$) to be 0.37 ± 0.02 nM, which is similar to the K_D determined by equilibrium binding (0.46 nM). Thus, there is good agreement between equilibrium and kinetic binding parameters. By a similar analysis, we determined the kinetic binding parameters for $hA_{2A}AR$-$\alpha_s\beta_1\gamma_2$ complexes: $k_1 = 1.40 \times 10^8 \pm 0.12 \times 10^8$ min/M, k_{-1} = 0.0295 ± 0.003 min^{-1}, and K_D = 0.21 ± 0.06 nM. These values are not significantly different from those for $hA_{2A}AR$-$\alpha_s\beta_4\gamma_2$.

We also observed two affinity sites of the receptor based on competition binding assays with agonists. Figure 4 demonstrates that when ^{125}I-ZM241385 binds to membranes expressing the $hA_{2A}AR$ and G proteins, competition by the agonist, ATL 146e, for binding sites is biphasic. To accurately determine both K_i values from these biphasic curves, we used a curve-fitting algorithm that directly calculated both K_i values based on the K_D of the radioligand and correcting for the depletion of both the radioligand and the competing compound during binding (see *Experimental Procedures*). When fit to a two-site model, the competition curve yields two K_i values for the potent A_{2A} ligand ATL 146e: 0.18 and 58 nM. A comparison of [^{125}I]APE and ATL 146e reveals a potency difference of 2.6- and 2.1-fold, respectively, for the high- and low-affinity $hA_{2A}AR$ binding sites. Addition of GTPγS in competition assays completely eliminates the high-affinity K_i, leaving a low-affinity K_i (58 nM), which is consistent with the K_i for ATL 146e when competing for ^{125}I-ZM241385 binding sites in membranes expressing the receptor alone (68 nM, Table 2). The high-affinity K_i of ATL 146e in competition for ^{125}I-ZM241385 (0.18 nM) is not significantly different from the K_i calculated from competition for [^{125}I]APE (0.20 nM).

To determine the affinities of other adenosine receptor agonists at G protein-coupled A_{2A} receptors, we performed competition experiments using low concentrations (0.3–0.5 nM) of [^{125}I]APE as the radioligand. At the concentrations used, the radioligand was bound predominantly (>95%) to the high-affinity site. We chose several agonists that are widely used experimentally because they have been reported to be highly selective for binding to one of the four adenosine receptor subtypes: A_{2A}-selective, ATL146e and CGS21680; A_3 selective, IB-MECA and Cl-IBMECA; and A_1 selective, CPA and CCPA. We also examined the nonselective agonist, NECA. As expected, these agonists have a much higher affinity for the G protein coupled $hA_{2A}AR$ than for the A_{2A} receptor expressed without any G proteins. A typical experiment is shown in Fig. 5 and the results of 60 experiments are summarized in Table 2.

We also examined four antagonists in competition assays: theophylline, MRS1220, XAC, and ZM241385. The results are summarized in Table 3. The K_i values of antagonists do

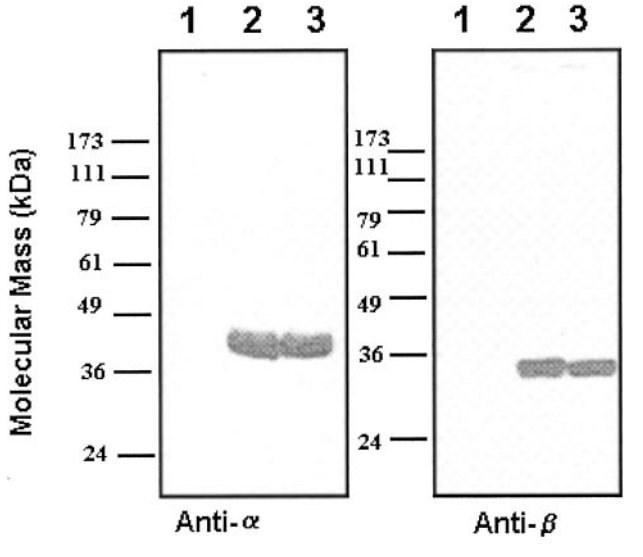

Fig. 1. Western blot for Gα (left) and Gβ (right) in membrane preparations of Sf9 cells infected with baculoviruses encoding the recombinant $hA_{2A}AR$ alone (lane 1), receptor plus α_s, β_1, and γ_2 (lane 2), or receptor plus α_s, β_4, and γ_2 (lane 3). Electrophoresis, transfer, and blotting were performed as described under *Experimental Procedures*. The result shown is typical of triplicate experiments.

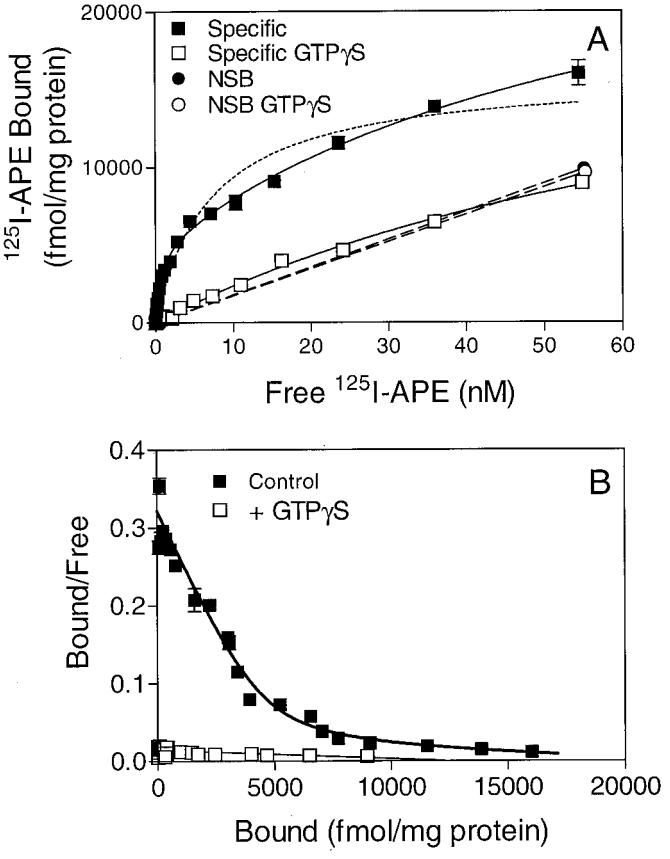

Fig. 2. [^{125}I]APE saturation binding to $hA_{2A}AR$-$\alpha_s\beta_4\gamma_2$ complexes. Sf9 cells were infected with recombinant baculoviruses expressing the human $A_{2A}AR$ and the G protein subunits α_s, β_4, and γ_2. Membranes were prepared 72 h after infection and radioligand binding was performed as described under *Experimental Procedures*. A, equilibrium binding of [^{125}I]APE in the absence (■) or presence (□) of GTPγS. Nonspecific binding was assayed by addition of saturating concentration (50 μM) NECA in the absence (●) or presence (○) of GTPγS. The solid line through solid squares represents a two-site fit of the equilibrium binding data, whereas the dotted line represents a one-site fit. B, Scatchard plot of equilibrium binding in the absence (■) or presence (□) of GTPγS. Binding parameters from triplicate experiments are summarized in Table 1.

not vary significantly between the coupled and uncoupled receptors. These results are consistent with the expectation that antagonists do not differ substantially in their affinities for coupled and uncoupled receptors.

To examine the selectivity of selected compounds for various adenosine receptor subtypes, we performed competition radioligand binding experiments to membranes expressing the human A_1AR or A_3AR using the agonist [^{125}I]ABA. At the [^{125}I]ABA concentrations used, >80% of radioligand binding in these systems is GTPγS sensitive and therefore predominantly represents the high-affinity binding sites of these receptors. Resultant competition curves were fit with both one- and two-site models. In all cases, the one-site model better fit the data as determined by F tests (Motulsky and Ransnas, 1987). K_i values were determined as described under *Experimental Procedures*. The high-affinity K_i values from these experiments are summarized in Table 4. We also calculated the selectivity ratio of each agonist at high-affinity A_1 and A_3 receptors relative to both their low and high A_{2A} affinities. The results indicate that agonists that are considered to be selective for A_1 or A_3 receptors are less selective over A_{2A} receptors than previously noted.

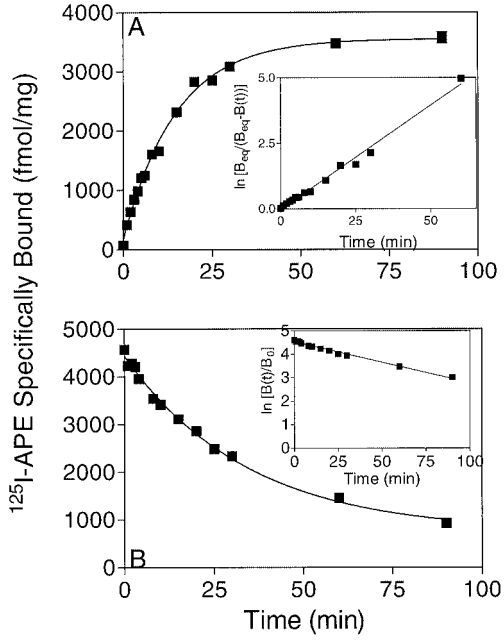

Fig. 3. Time courses of 0.34 nM [^{125}I]APE association with and dissociation from A_{2A}AR-$\alpha_s\beta_4\gamma_2$ complexes. Sf9 cells were infected with recombinant baculoviruses expressing the human A_{2A}AR and the G protein subunits α_s, β_4, and γ_2. Membranes were prepared 72 h after infection and radioligand binding was performed as described under *Experimental Procedures.* A, specific binding of [^{125}I]APE at time *t* after addition of radiolabeled agonist to membranes. Inset, a linear regression of transformed data. B, specific binding of [^{125}I]APE at time *t* after dissociation is induced by addition of saturating antagonist (50 μM ZM241385) to radioligand/membrane solution which had be incubated for 3 h. Inset, log transformation of the data in B with a linear regression of the transformed data, illustrating dissociation from a single site. The data shown is typical of three to five experiments.

Discussion

We have developed a system in which the G protein-coupled state of the A_{2A}AR can be accurately detected using a quadruple infection of Sf9 cells with baculoviruses encoding the hA_{2A}AR and three G protein subunits. Previous studies using transfected COS-7 cells (Piersen et al., 1994) or HEK293 cells (Rieger et al., 2001; Sullivan et al., 2001) display little or no GTPγS-sensitive agonist binding, possibly because of the low levels of G_s expressed in these cell lines relative to the highly expressed receptor or to other factors that limit coupling of receptors to G_s.

In this study, we show that the identity of the β subunit can influence the coupling efficiency of the A_{2A}AR. Overexpressing $\alpha_s\beta_1\gamma_2$ with the A_{2A}AR in Sf9 cells resulted in only partially coupled A_{2A}AR (8%), but substantially greater coupling was observed (40%) if β_1 was replaced by β_4. This difference was not due to variations in protein expression levels as determined by Western blots. The results are consistent with the recent report showing in reconstitution ex-

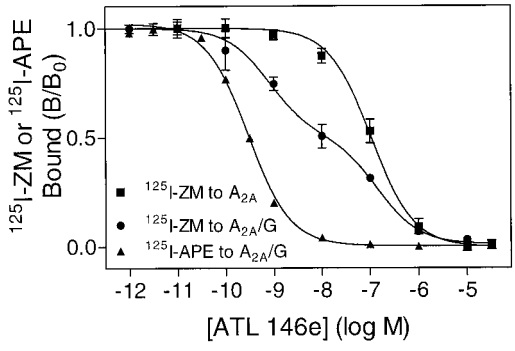

Fig. 4. Competition of ATL 146e for binding sites on hA_{2A}AR. Binding is plotted as a fraction of control specific binding. Data for ATL 146e competition for ^{125}I-ZM241385 binding on Sf9 membranes expressing the A_{2A} receptor alone (■) (K_i = 68 nM) or A_{2A}AR-$\alpha_s\beta_4\gamma_2$ complexes (●) ($K_{i,H}$ = 0.18 nM and $K_{i,L}$ = 58 nM) and [^{125}I]APE binding on membranes expressing A_{2A}AR-$\alpha_s\beta_4\gamma_2$ complexes (▲) (K_i = 0.20 nM) are representative of three to six replicate experiments.

TABLE 2

Comparison of high- and low-affinity K_i values for selected agonist compounds at the hA_{2A}AR

K_{iL} (expressed as mean ± S.E.M.) values were determined from the IC_{50} of the agonist in competition with ^{125}I-ZM241285 on A_{2A} receptors expressed in Sf9 cells. High-affinity K_{iH} values were determined from the IC_{50} of the drug in competition with [^{125}I]APE on A_{2A} receptors expressed with heterotrimeric G proteins (α_s,β_4,γ_2) in Sf9 cells.

	Low Affinity ($K_{i,L}$)	*n*	High Affinity ($K_{i,H}$)	*n*	Low/High
	nM		*nM*		
ATL 146e	67.9 ± 10	4	0.20 ± 0.02	6	340
[^{125}I]APE	26 ± 6	3	0.46 ± 0.1	3	57
CGS 21680	944 ± 200	3	4.9 ± 0.20	5	192
NECA	84.7 ± 38	5	2.0 ± 0.20	4	42
IB-MECA	5,429 ± 1,070	3	6.3 ± 0.80	3	862
CI-IBMECA	7,692 ± 980	3	18.3 ± 3.2	4	420
CCPA	5,466 ± 293	3	11.0 ± 1.9	4	497
CPA	10,370 ± 350	3	19.8 ± 3.2	4	523

n, number of independent experiments done in triplicate.

periments that β_4 is significantly more potent than β_1 in stimulating agonist-induced guanine nucleotide exchange in Sf9 membranes expressing $hA_{2A}AR$ (McIntire et al., 2001). Our data imply that the difference in guanine nucleotide exchange is a consequence of changes in the stability of the agonist-receptor-G protein complex, which is dependent on the composition of the Gβ subunit. Gβ composition also influences the coupling of M_2 muscarinic receptors such that guanine nucleotide exchange on $\alpha_o\beta_4\gamma_2$ is greater than on $\alpha_o\beta_1\gamma_2$ (Hou et al., 2001). The influence of G protein composition on A_{2A} receptor coupling has not been as extensively studied as the A_1 receptor. A_1 receptors couple preferentially to G proteins containing γ_2 or γ_3 over subunits that contain γ_1 (Figler et al., 1997). Additional experimentation will be required to determine whether, like the A_1 receptor, the coupling of A_{2A} receptors is influenced by the composition of Gγ.

We used $\alpha_s\beta_4\gamma_2$ to carefully examine the high-affinity binding site of $hA_{2A}ARs$. Several lines of evidence support the conclusion that the high-affinity binding site observed in this study results from G protein coupling: 1) the agonist used ([^{125}I]APE) was previously shown to bind to both coupled and uncoupled $A_{2A}AR$ receptors on rat striatal membranes (Luthin et al., 1995); 2) two affinity states were detected in both saturation and competition studies; 3) high-affinity binding to quadruply infected Sf9 membranes was completely inhibited by the addition of 50 μM GTPγS to binding assays; 4) the high-affinity site was absent in membranes expressing the receptor alone; and 5) agonists, but not antagonists, bound differentially to coupled and uncoupled receptors.

It is significant that agonist radioligands of the A_{2A} receptor such as [^{125}I]APE and the widely used compound [^{3}H]CGS21680 bind with high enough affinity to detect both uncoupled and coupled receptors. Consequently, attempts to fit radioligand binding data to a single site may result in detection of a composite apparent binding site that is intermediate in its affinity for coupled and uncoupled receptors. This will result in discrepancies in agonist binding constants that depend on various factors, including the receptor density, the fraction of coupled receptors, the concentration of radioligand, and the time and temperature of filter washing. The absolute affinity of the radioligand for the low-affinity site will influence its detection because the lowest affinity ligands are most prone to washing off the receptor during the wash phase of the filtration process. In this regard, it is notable that the rank affinity of agonists radioligands for the low-affinity site is: [^{125}I]APE (26 nM) < [^{3}H]NECA (85 nM) < [^{3}H]CGS21680 (944 nM). Collectively, this may explain the wide differences in reported agonist binding affinities for the A_{2A} receptors between laboratories and the fact that the high-affinity K_i values found in this study are significantly lower than those reported previously (Robeva et al., 1996; Klotz et al., 1998) because previous studies have not had the benefit of a well-coupled receptor system and thus could not explicitly detect the high-affinity state.

We measured both the low- and high-affinity K_i values of several widely used adenosine receptor agonists. It is notable that the ratio of binding affinity for the high- and low-affinity sites was highly variable among the agonists we examined and ranged from 862-fold with IB-MECA to 42-fold with NECA (Table 2). This is a significant observation because it indicates that even the relative affinities and rank order potency of agonists vary depending on the coupling state of receptors. Stated another way, these data indicate that binding to uncoupled A_{2A} receptors is not highly predictive of binding to coupled receptors. The reason for the variance in the ratio between high- and low-affinity K_i values is interesting and is the subject of ongoing work in our laboratory.

For comparing the selectivity of agonists for the four adenosine receptor subtypes, it makes sense to compare coupled receptors to coupled receptors, or uncoupled receptors to uncoupled receptors. In contrast to recombinant $hA_{2A}ARs$, recombinant hA_1ARs and hA_3ARs do couple sufficiently well to G proteins to readily allow detection of the high-affinity agonist binding conformation characterized by agonist binding that is largely inhibited by GTPγS (Gao et al., 1999). This may be related to the fact that $G_{i/o}$ is more abundant in mammalian cells than is G_s. In addition, the $G_{i/o}$ proteins seem to couple very tightly to their cognate receptors (Munshi et al., 1991; Gao et al., 1999). Consequently, the selectivity of agonists has been assessed in many instances based on competition of radioligand binding to well-coupled A_1 and A_3 receptors, but to poorly coupled A_{2A} receptors. Based on a comparison of well-coupled A_1, A_{2A}, and A_3 receptors, we have shown in this study that among agonists generally used as A_{2A}-selective ligands (ATL146e and CGS21680), the limited apparent selectivity for human A_{2A} receptors is actually substantially higher than previously thought (Sullivan et al., 2001). Moreover, the high-affinity K_i values for agonists in our experiments are more in line with their functional EC_{50} values in other studies (Walker et al., 1997; Sullivan et al.,

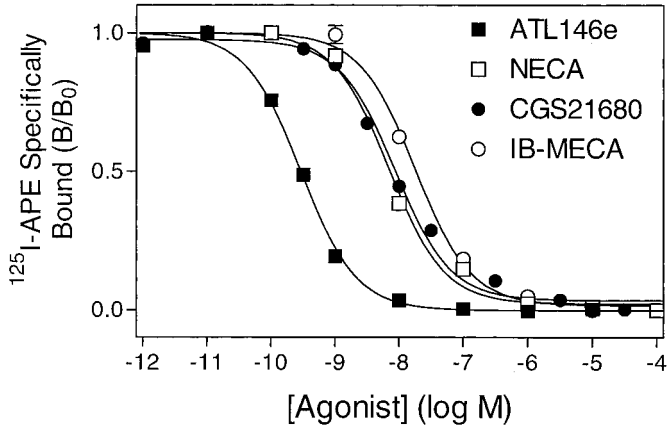

Fig. 5. Competition of adenosine receptor agonists for [^{125}I]APE binding to $A_{2A}AR$-$\alpha_s\beta_4\gamma_2$ complexes. Binding is plotted as a fraction of control specific binding. Data for ATL 146e (■), NECA (□), CGS 21680 (●), and IB-MECA (○) are shown. The data was fit by nonlinear regression to a one-site binding model. Binding parameters from replicate experiments are summarized in Table 2.

TABLE 3
Affinity of antagonists for coupled and uncoupled $hA_{2A}AR$
High- and low-affinity K_i values are expressed as mean ± S.E.M. for selected antagonist compounds. Values were determined as described under *Experimental Procedures.*

Radioligand	^{125}I-ZM241385 on $hA_{2A}AR$	*n*	[^{125}I]APE on $hA_{2A}AR$-$\alpha_s\beta_{4\gamma2}$	*n*
	nM		*nM*	
MRS 1220	13.3 ± 1.9	3	15 ± 1.0	5
Theophylline	10,900 ± 1,500	3	9,500 ± 723	4
XAC	10.9 ± 0.9	3	12.9 ± 0.4	5
ZM241385	1.0 ± 0.1	3	1.6 ± 0.1	5

n, number of independent experiments done in triplicate.

TABLE 4

Selectivity of adenosine ligands for G protein coupled A_1, A_{2A}, and A_3 receptors

K_i values (expressed as mean ± S.E.M. n = 3–5) were determined from IC_{50} values of the agonists in competition with [^{125}I]ABA as described under *Experimental Procedures*. Potency ratios were calculated by dividing the high- or low-affinity K_i at the A_{2A}AR by the high affinity K_i at the A_1 or A_3 AR.

		Potency Ratio			Potency Ratio	
	A_1K_i	$A_1/A_{2A\text{-high}}$	$A_1/A_{2A\text{-low}}$	A_3K_i	$A_3/A_{2A\text{-high}}$	$A_3/A_{2A\text{-low}}$
	nM			*nM*		
ATL 146e	77 ± 12	0.0026	1	45 ± 15	0.0044	1.72
CGS21680	316 ± 59	0.016	3	82 ± 18	0.059	11.5
NECA	2.0 ± 1.4	1	43	32 ± 9	0.063	2.6
CI-IBMECA	33 ± 9	0.56	238	2.4 ± 0.3	7.7	3,250
IB-MECA	9.0 ± 0.8	0.71	625	1.5 ± 0.3	4.2	3,570
CCPA	0.3 ± 0.1	33	18,200	65 ± 6	0.17	83
CPA	0.4 ± 0.1	50	26,600	93 ± 7	0.2	111

2001) than the low-affinity K_i values determined here and by others.

We also examined agonists reported be highly A_1 and A_3 selective. We confirmed that the radioligand binding in these assays is to a single GTPγS-sensitive site. CCPA and CPA both have subnanomolar affinities for the coupled A_1AR and have been described as highly selective agonists of the A_1 receptor. Previous studies have cited selectivity ratios for A_1 over A_{2A} receptors of over 300-fold for CPA and over 2000-fold for CCPA (Klotz et al., 1998). However, in this study we have shown that both of these compounds have only a 30- to 50-fold selectivity for A_1 over A_{2A} at their high-affinity binding sites. This finding would seem to explain the effect of CCPA to increase interleukin-10 release and decrease tumor necrosis factor-α concentrations in endotoxemic mice at high concentrations (Hasko et al., 1996), actions that have been shown to be A_{2A} dependent in vitro (Bouma et al., 1994; Sullivan and Linden, 1998).

Similarly, examination of the high-affinity K_i values for IB-MECA and Cl-IB-MECA shows that neither is as selective for A_3 over A_{2A} receptors as has been reported (Gallo-Rodriguez et al., 1994; Klotz et al., 1999). Both of these agonists have only a ~5-fold selectivity for A_3 over A_{2A} for binding to the high-affinity site. This finding has critical importance for work involving discrimination of the physiological roles of the A_3 and A_{2A}ARs in mediating the protective effects of adenosine. Various groups have relied on IB-MECA to define the role that the A_3AR receptor plays modulating inflammatory responses (Hasko et al., 1996, 1998; Sajjadi et al., 1996). This was reasonable based on the relative potencies of these compounds reported in the prior literature. However, because the A_{2A} and A_3AR work through opposing mechanisms ($G\alpha_s$ versus $G\alpha_i$), it seems unlikely that both receptors could have the generally anti-inflammatory effects noted in the same cells. The potency of IB-MECA at the A_{2A}AR confirms our recent observation that the anti-inflammatory effects of IB-MECA on tumor necrosis factor-α production in human monocytes can be potently blocked by the selective A_{2A} antagonist, ZM241385 (Sullivan and Linden, 1998).

Comparing K_i values of compounds is an excellent method for determining selectivity of agonist binding at various receptors. However, this does not give a complete picture of agonist action because these values do not incorporate the efficacy of the various agonists at each receptor. A given agonist could have equal potencies at two given receptors, but if its efficacy at one is much greater than at the other, the agonist would seem to be more potent at one receptor in functional assays. Because no work has been published on the relative efficacies of these compounds, we do not yet have a complete understanding of these agonists' actions.

In summary, we report here on the establishment of a method for expressing G protein coupled hA_{2A}ARs by quadruple infection of Sf9 cells and sensitivity of this coupling to Gβ composition. We have confirmed the existence of this high-affinity state by Scatchard analysis, competition assays, and kinetic experiments. Using this system, we have determined the affinity of several commonly used adenosine receptor agonists at the coupled A_{2A}AR. This work has demonstrated that IB-MECA and Cl-IB-MECA can no longer be assumed to be highly selective agonists of the hA_3AR or CCPA, a highly selective agonist of the hA_1AR. Consequently, findings based on the use of these agonists must be critically evaluated with respect to possible involvement of the A_{2A}AR in responses that have been previously ascribed to A_1 or A_3 receptors. We anticipate that the use of methods to express well coupled adenosine receptors will be valuable for detecting novel potent and selective AR agonists.

Acknowledgments

We gratefully acknowledge Dr. James Garrison of the University of Virginia for his generous gift of baculoviruses for G protein subunits, Dr. Ken Jacobson of the National Institute of Diabetes and Digestive and Kidney Diseases for his gift of MRS1220 and Simon Poucher of Astra-Zeneca for his gift of ZM241385. We also thank Dr. William McIntire and Heidi Figler for helpful advice.

References

Bouma MG, Stad RK, Van den Wildenberg FAJM, and Buurman WA (1994) Differential regulatory effects of adenosine on cytokine release by activated human monocytes. *J Immunol* **153:**4159–4168.

Figler RA, Lindorfer MA, Graber SG, Garrison JC, and Linden J (1997) Reconstitution of bovine A_1 adenosine receptors and G proteins in phospholipid vesicles: betagamma-subunit composition influences guanine nucleotide exchange and agonist binding. *Biochemistry* **36:**16288–16299.

Gallo-Rodriguez C, Ji X, Melman N, Siegman BD, Sanders LH, Orlina J, Fischer B, Pu Q, Olah ME, Van Galen PJM, et al. (1994) Structure-activity relationships of N^6-benzyladenosine- 5′-uronamides as A_3-selective adenosine agonists. *J Med Chem* **37:**636–646.

Gao Z, Robeva AS, and Linden J (1999) Purification of A1 adenosine receptor-G-protein complexes: effects of receptor down-regulation and phosphorylation on coupling. *Biochem J* **338:**729–736.

Hasko G, Nemeth ZH, Vizi ES, Salzman AL, and Szabo C (1998) An agonist of adenosine A3 receptors decreases interleukin-12 and IFN-γ production and prevents lethality in endotoxemic mice. *Eur J Pharmacol* **358:**261–268.

Hasko G, Szabo C, Nemeth ZH, Kvetan V, Pastores SM, and Vizi ES (1996) Adenosine receptor agonists differentially regulate IL-10, TNF-alpha, and nitric oxide production in RAW 264.7 macrophages and in endotoxemic mice. *J Immunol* **157:**4634–4640.

Hou YM, Chang V, Capper AB, Taussig R, and Gautam N (2001) G protein beta subunit types differentially interact with a muscarinic receptor but not adenylyl cyclase type II or phospholipase C-beta 2/3. *J Biol Chem* **276:**19982–19988.

Jacobson KA (1998) Adenosine A3 receptors: novel ligands and paradoxical effects. *Trends Pharmacol Sci* **19:**184–191.

Klotz K-N, Hessling J, Hegler J, Owman C, Kull B, Fredholm BB, and Lohse MJ (1998) Comparative pharmacology of human adenosine receptor subtypes—characterization of stably transfected receptors in CHO cells. *Naunyn-Schmiedeberg's Arch Pharmacol* **357:**1–9.

Klotz KN, Camaioni E, Volpini R, Kachler S, Vittori S, and Cristalli G (1999) 2-substituted *N*-ethylcarboxamidoadenosine derivatives as high-affinity agonists at human A3 adenosine receptors. *Naunyn-Schmiedeberg's Arch Pharmacol* **360:** 103–108.

Linden J (1982) Calculating the dissociation constant of an unlabeled compound from the concentration required to displace radiolabel binding by 50%. *J Cyclic Nucleotide Res* **8:**163–172.

Linden J (2001) Molecular approach to adenosine receptors: receptor-mediated mechanisms of tissue protection. *Annu Rev Pharmacol Toxicol* **41:**775–787.

Linden J, Patel A, and Sadek S (1985) [^{125}I]Aminobenzyladenosine, a new radioligand with improved specific binding to adenosine receptors in heart. *Circ Res* **56:**279–284.

Linden J, Patel A, Spanier AM, and Weglicki WB (1984) Rapid Agonist-induced decrease of ^{125}I-pindolol binding to beta-adrenergic receptors. Relationship to desensitization of cyclic AMP accumulation in intact heart cells. *J Biol Chem* **259:**15115–15122.

Linden J, Taylor HE, Robeva AS, Tucker AL, Stehle JH, Rivkees SA, Fink JS, and Reppert SM (1993) Molecular cloning and functional expression of a sheep A_3 adenosine receptor with widespread tissue distribution. *Mol Pharmacol* **44:**524–532.

Luthin DR, Olsson RA, Thompson RD, Sawmiller DR, and Linden J (1995) Characterization of two affinity states of adenosine A_{2A} receptors with a new radioligand, 2-[2-(4-amino-3- [^{125}I]iodophenyl)ethylamino]adenosine. *Mol Pharmacol* **47:**307–313.

Marquardt DM (1963) An algorithm for least-squares estimation of nonlinear parameters. *J Soc Indust Appl Math* **11:**431–441.

McIntire WE, MacCleery G, and Garrison JC (2001) The G protein β subunit is a determinant in coupling of the G_s β subunit to the β adrenergic and A_{2A} adenosine receptors. *J Biol Chem* **276:**15801–15809.

Motulsky HJ and Ransnas LA (1987) Fitting curves to data using nonlinear regression: a practical and nonmathematical review. *FASEB J* **1:**365–374.

Munshi R, Pang I-H, Sternweis PC, and Linden J (1991) A_1 adenosine receptors of bovine brain couple to guanine nucleotide-binding proteins G_{i1}, G_{i2}, and G_0. *J Biol Chem* **266:**22285–22289.

Piersen CE, True CD, and Wells JN (1994) A carboxyl-terminally truncated mutant and nonglycosylated A_{2a} adenosine receptors retain ligand binding. *Mol Pharmacol* **45:**861–870.

Poucher SM, Keddie JR, Singh P, Stoggall SM, Caulkett PW, Jones G, and Coll MG (1995) The in vitro pharmacology of ZM 241385, a potent, nonxanthine A_{2A} selective adenosine receptor antagonist. *Br J Pharmacol* **115:**1096–1102.

Rieger JM, Brown ML, Sullivan GW, Linden J, and MacDonald TL (2001) Design, synthesis, and evaluation of novel adenosine A_{2A} receptor agonists. *J Med Chem* **44:**531–539.

Robeva AS, Woodard R, Luthin DR, Taylor HE, and Linden J (1996) Double tagging recombinant A_1- and A_{2A}-adenosine receptors with hexahistidine and the FLAG epitope. Development of an efficient generic protein purification procedure. *Biochem Pharmacol* **51:**545–555.

Rosin DL, Woodard RL, Guyenet PG, and Linden J (1996) Distribution of A_{2A} adenosine receptors (A_{2A}ARs) in rat brain: characterization of monoclonal antibodies and immunohistochemical localization of A_{2A}ARs. *Soc Neurosci Abstr* **22:** 616.

Sajjadi FG, Takabayashi K, Foster AC, Domingo RC, and Firestein GS (1996) Inhibition of TNF-alpha expression by adenosine: role of A_3 adenosine receptors. *J Immunol* **156:**3435–3442.

Sullivan GW and Linden J (1998) Role of A_{2A} adenosine receptors in inflammation. *Drug Dev Res* **45:**103–112.

Sullivan GW, Linden J, Buster BL, and Scheld WM (1999) Neutrophil A_{2A} adenosine receptor inhibits inflammation in a rat model of meningitis: synergy with the type IV phosphodiesterase inhibitor, rolipram. *J Infect Dis* **180:**1550–1560.

Sullivan GW, Rieger JM, Scheld WM, MacDonald TL, and Linden J (2001) Cyclic AMP-dependent inhibition of human neutrophil oxidative activity by substituted 2-propynylcyclohexyl adenosine A_{2A} receptor agonists. *Br J Pharmacol* **132:**1017–1026.

Walker BA, Rocchini C, Boone RH, Ip S, and Jacobson MA (1997) Adenosine A_{2A} receptor activation delays apoptosis in human neutrophils. *J Immunol* **158:**2926–2931.

Wennmalm M (1988) Effect of hypoxia on nerve-stimulation-induced release of noradrenaline from the rabbit heart. *Acta Physiol Scand* **133:**25–33.

Address correspondence to: Dr. Joel Linden, UVA Health System, PO Box 801395, Charlottesville, VA 22908. E-mail: jlinden@virginia.edu